

Size-Dependent Spintronic Properties of Dilute Magnetic Semiconductor Nanocrystals

Xiangyang Huang,¹ Adi Makmal,² James R. Chelikowsky,¹ and Leeor Kronik²

¹*Department of Chemical Engineering and Materials Science, Institute for the Theory of Advanced Materials in Information Technology, Digital Technology Center, University of Minnesota, Minneapolis, Minnesota 55455, USA*

²*Department of Materials and Interfaces, Weizmann Institute of Science, Rehovoth 76100, Israel*

(Received 28 December 2004; published 13 June 2005)

The electronic structure and magnetic properties of Mn-doped Ge, GaAs, and ZnSe nanocrystals are investigated using real space *ab initio* pseudopotentials constructed within the local spin-density approximation. The ferromagnetic and half-metallicity trends found in the bulk are preserved in the nanocrystals. However, the Mn-related impurity states become much deeper in energy with decreasing nanocrystalline size, causing the ferromagnetic stabilization to be dominated by double exchange via localized holes rather than by a Zener-like mechanism.

DOI: 10.1103/PhysRevLett.94.236801

PACS numbers: 73.20.Hb, 73.21.La, 73.22.-f, 78.67.-n

Two exciting developments in semiconductor science and technology are the advent of dilute magnetic semiconductors (DMSs) and of semiconductor nanocrystals (NCs). DMSs are semiconductors to which a magnetic impurity has been intentionally introduced. They have attracted considerable attention because they exhibit unique magnetic, magneto-optical, and magneto-electrical effects. They also hold the promise of using electron spin, in addition to charge, for creating a new class of “spintronic” semiconductor devices [1]. Semiconductor nanoparticles have been studied intensively because of their unusual electronic and optical properties, which may differ fundamentally from those of the corresponding bulk material. Of particular appeal is that the properties of NCs can be radically altered, while maintaining their chemical composition, simply by changing their size and/or shape [2].

It is important to understand the role of dimensionality in shaping the spin-polarized electronic structure of nanocrystalline DMS [1,3] because quantum confinement may result in intriguing magnetic properties. Furthermore, magnetic dots have been suggested for use in quantum computation [4] and spin communication between semiconducting nanoparticles has been demonstrated [5]. Despite this importance, no systematic study of the electronic structure of Mn-containing nanocrystalline DMS from first principles has been undertaken. We are aware of only one paper where size effects, on a particular DMS ($\text{Mn}_x\text{Ga}_{1-x}\text{As}$), have been examined theoretically [6].

We present calculations for the electronic structure and magnetic properties of Mn-containing Ge, GaAs, and ZnSe nanoparticles. All three are well-known semiconductors, which are prototypical of group IV, III-V, and II-VI semiconductors. The elements comprising these semiconductors are found in the same row of the periodic table and these semiconductors have the same (zinc blende/diamond) crystalline structure, making an identification of chemical trends easier. Mn-based bulk DMS have been successfully synthesized in all three cases [7–9] and a successful synthesis of high-quality Mn-containing ZnSe NCs has been reported [10].

NCs were constructed by taking spherical fragments of the corresponding bulk material. We passivated the Ge surface using hydrogens, whereas the surfaces of GaAs and ZnSe were passivated using fictitious, hydrogenlike atoms with fractional charge [11]. Because magnetic circular dichroism experiments have suggested that each NC contains, on average, one Mn atom [10], we chose to study the effects of placing one or two Mn atoms inside the crystal. A fourfold coordinated Mn atom was placed in the center of the Ge NC. In GaAs and ZnSe, the Mn atom was substituted on a cation site in the center of the NC. We considered four Mn-doped NCs: $X_9\text{MnY}_{10}$, $X_{18}\text{MnY}_{19}$, $X_{40}\text{MnY}_{41}$, and $X_{64}\text{MnY}_{65}$, where $X = \text{Ge, Ga, or Zn}$ and $Y = \text{Ge, As, or Se}$, respectively. The passivation atoms are implicit. These cases correspond to effective Mn concentrations of 5%, 2.63%, 1.22%, and 0.77%, respectively. We additionally examined Mn-Mn interactions by considering two Mn atoms that were placed such that they were bridged by an anion atom. For the Ge NC, we examined a nearest-neighbor Mn dimer.

We determined the electronic structure of these systems using pseudopotentials constructed within the local spin-density approximation of density functional theory [12]. The Kohn-Sham equations were solved on a real space grid using a higher-order finite difference method [13]. A grid spacing of 0.4 a.u. and a separation of at least 5 a.u. between the outermost passivating atoms and a spherical boundary were used throughout.

Figure 1 shows the total valence charge density ($\rho_+ + \rho_-$) and spin-density ($\rho_+ - \rho_-$) contour plots for the 82-atom NC containing one Mn atom. In all cases, the charge density maps show Mn bonding with its nearest neighbors, indicating hybridization between Mn *d* and anion *s-p* states. The spin-density maps indicate a strongly localized magnetic moment at the Mn site. For the Ge and GaAs NCs, the spin polarization of the atoms nearest to the Mn atom has an opposite sign to that of Mn. The spin-density distribution along the Mn-As or Mn-Ge bond shows a *p* character. Its opposite spin sign is a signature of antiferromagnetic (AFM)

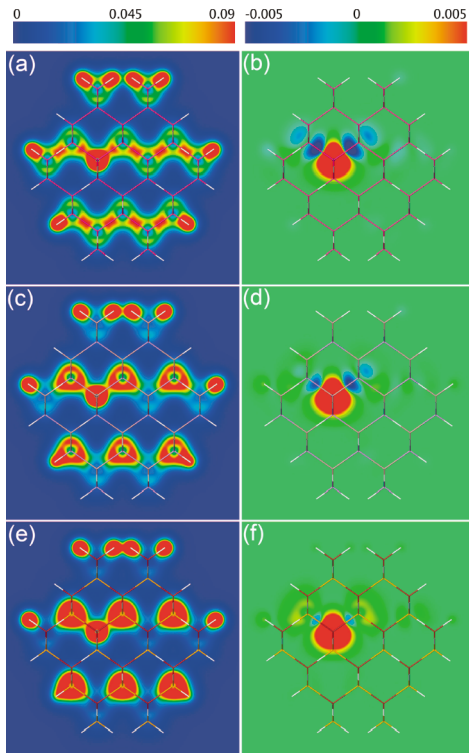


FIG. 1 (color). Total valence charge density (a), (c), (e) and spin density (b), (d), (f) for passivated Ge_{81}Mn , $\text{Ga}_{40}\text{MnAs}_{41}$, and $\text{Zn}_{40}\text{MnSe}_{41}$ nanocrystals, respectively.

coupling between the Mn atom and surrounding charge carriers.

Figure 2 shows the spin-polarized energy levels for the 82-atom systems. In all cases, the gap states are derived from Mn $3d$ states and reflect the splitting of the $3d$ states by the T_d crystal field to an e doublet and a t_2 triplet. As expected for T_d symmetry [14], the e levels have a lower energy than the t_2 levels in both spin channels. An analysis

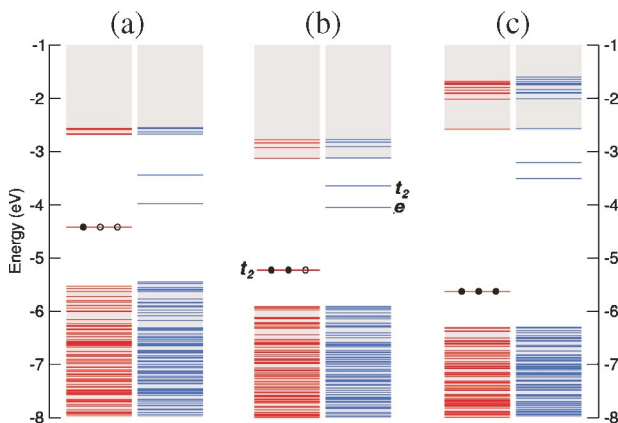


FIG. 2 (color). Spin-polarized electronic structure for passivated (a) Ge_{81}Mn , (b) $\text{Ga}_{40}\text{MnAs}_{41}$, and (c) $\text{Zn}_{40}\text{MnSe}_{41}$ nanocrystals. The e and t_2 levels are doubly and triply degenerate, respectively. The Fermi level is located at the majority spin t_2 levels in all cases. Filled and empty circles denote electrons and holes, respectively. The majority levels are shown in red.

of the corresponding wave functions shows that the valence band edge is comprised mainly of anion p states. The majority spin e levels are fully occupied, hybridized with anion p states, and located right below (~ 0.05 eV) the valence band edge in all three materials. The majority t_2 levels are characterized by a certain amount of hybridization with the four neighboring p orbitals and the corresponding charge density is highly localized on the MnY_4 complex.

Previous calculations have shown that bulk Ge:Mn [15,16] and GaAs:Mn [17,18] are half-metallic, but bulk ZnSe:Mn is semiconducting [19]. The origins of this behavior are apparent here. Figure 2 shows that the e and t_2 minority spin levels are empty, so that the minority spin retains its semiconducting nature even with the Mn impurity in all three cases. However, the highest occupied molecular orbitals t_2 level of the majority spin is partially occupied for Ge:Mn and GaAs:Mn, but it is fully occupied for ZnSe:Mn. This configuration is in agreement with a “half-metallic” nature of majority spin electrons for Ge and GaAs and a semiconducting nature for ZnSe.

The introduction of the Mn impurity does not change the number of minority spin *occupied* states. Therefore, the introduction of the five Mn d electrons results in a net magnetic moment of $3\mu_B$, $4\mu_B$, and $5\mu_B$ for Ge, GaAs, and ZnSe, respectively. This is in agreement with the magnetic moment of $5\mu_B$ for the free Mn atom being modified by the doubly ionized acceptor, singly ionized acceptor, and iso-electronic nature of Mn in Ge, GaAs, and ZnSe, respectively. A similar picture applies to the corresponding bulk DMS [20]. The loss of two p electrons when Mn replaces a Ge atom but only one when it replaces a Ga atom immediately explains why the spin polarization is more pronounced in Ge than in GaAs in the spin-density maps of Fig. 1.

In principle, the partially occupied degenerate t_2 levels of the Ge:Mn and GaAs:Mn should display a Jahn-Teller effect. We have not studied this effect here. However, studies of bulk GaAs:Mn [21] and Ge:Mn [22] suggest that it is negligibly small.

Our analysis for these NCs indicates that the qualitative level splitting and magnetic moment picture is similar to that of the bulk. This is due to the short-range interaction of Mn with its neighbors. However, there remain significant differences between the electronic structure of the bulk and of the NCs, due to quantum size effects, i.e., the increase of the semiconductor gap with decreasing NC size [2]. The differences are summarized in Fig. 3. We show in this figure the evolution of the “host gap” [i.e., the highest occupied molecular orbital (HOMO)–lowest unoccupied molecular orbital (LUMO) separation of states *not* derived from the Mn d orbitals], the “HOMO (host)” \uparrow – t_2^\downarrow separation, and the t_2^\uparrow – e^\downarrow (or $4T_1$ – $6A_1$) separation as a function of the NC diameter. All three energy separations exhibit a quantum size effect; however, this effect is very pronounced for the first, less pronounced for the second, and very small for the third. This is because the Mn-related

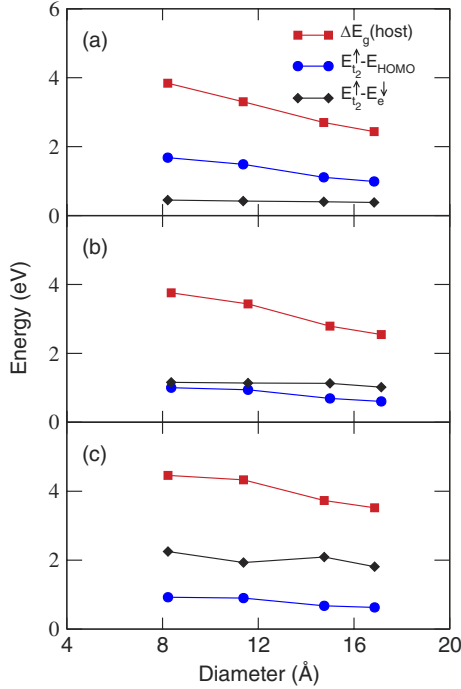


FIG. 3 (color online). Energy separation of host HOMO and LUMO (squares), host HOMO $\uparrow - t_2^{\uparrow}$ (circles), and $t_2^{\uparrow} - e^{\downarrow}$ (diamonds) as a function of nanocrystalline diameter for (a) Ge:Mn, (b) GaAs:Mn, and (c) ZnSe:Mn.

orbitals are more localized than those of the host. The more delocalized the levels are the greater the effect of confinement. The host gap only involves delocalized levels and exhibits large energy shifts; the HOMO(host) $\uparrow - t_2^{\uparrow}$ gap involves one delocalized orbital and exhibits moderate energy shifts; and the $t_2^{\uparrow} - e^{\downarrow}$ involves two localized orbitals and exhibits small energy shifts.

We have chosen the $t_2^{\uparrow} - e^{\downarrow}$ as representative of transitions between localized orbitals because in ZnSe:Mn the transition from the e^{\downarrow} levels to the t_2^{\uparrow} levels has been studied experimentally using photoluminescence. Its size dependence has been found to be weak [10]. Figure 3 shows that the $t_2^{\uparrow} - e^{\downarrow}$ energy separation changes from 2.25 to 1.81 eV as the NC size increases from 20 to 130 atoms. This range is close to the bulk value of 1.6 eV [19]. The experimental photoluminescence energy is higher (~ 2.1 eV [10]) than our calculated values—a well-known consequence of using the Kohn-Sham eigenvalues to predict excited state properties [23] that should not change the qualitative size trends.

The strong localization of the Mn impurity levels in the MnY_4 complex implies that the choice of the Mn position within the NC should not affect its electronic structure, as long as the Mn is not close to the surface. Our calculations for the 130-atom ZnSe:Mn case show an impurity level shift of less than 0.05 eV for different Mn positions.

The significantly different quantum size effects experienced by localized and delocalized orbitals have profound implications for the resulting electronic structure. In all

cases shown in Fig. 3, the minority e and t_2 levels are well within the host gap. In contrast, the same levels in the corresponding bulk systems are well within the conduction band [16,18]. The delocalized empty levels are pushed up in energy far more rapidly with decreasing size, eventually crossing the localized Mn-related levels.

A greater effect is found when examining the filled (“valence band”) states of the NC. In bulk GaAs, the valence band is well-known to exhibit a significant spin-splitting upon introduction of Mn [17]. No such splitting is found here, even for the 20-atom NC, where the Mn concentration is $\sim 5\%$, which is comparable to bulk Mn concentrations. The significant bulk-splitting in GaAs:Mn has been attributed to the fact that Mn is a shallow acceptor [24] and can strongly interact with the valence band [25]. For the 130-atom NC, the Mn t_2 states are ~ 0.6 eV above the “host HOMO”, because the delocalized occupied orbitals are pushed down in energy more rapidly than the Mn states with decreasing size [6]. This makes the Mn a deep acceptor, weakening the interaction and preventing spin-splitting of the occupied states. Only in the Ge:Mn NC do we see spin-splitting of the occupied states, consistent with the stronger Mn-host spin interaction shown in Fig. 1.

We introduced two Mn atoms into each 82-atom NC and considered the case where both Mn atoms are placed on adjacent cation sites, bridged through an anion (or in Ge, through a Ge atom). We compared the total energy differences between the ferromagnetic (FM, parallel spins) and antiferromagnetic (AFM, antiparallel spins) configurations. We found the FM structure to be more stable by 0.42 and 0.38 eV for Ge and GaAs, respectively, but less stable by 0.14 eV for ZnSe. This is in agreement with bulk results, where the stable phase of Ge:Mn and GaAs:Mn is predicted to be the FM one, whereas in ZnSe:Mn the stable phase is the AFM one. Also in agreement with bulk studies [26] is the fact that if both Mn atoms are nearest neighbors (i.e., they form a dimer) in Ge:Mn, the AFM phase is always more stable.

In the bulk, ferromagnetism in GaAs:Mn is ascribed to a Zener-like picture of mediation by free holes [27]. Ferromagnetism in Ge:Mn has been explained either within a similar Zener-like picture [26] or within a Ruderman-Kittel-Kasuya-Yosida (RKKY) picture of interaction with free carriers [15]. However, Fig. 2 clearly shows the absence of either free holes in the valence band or a metal-like presence of free carriers, which precludes either mechanism in the present case (the electronic structure diagram of the FM NC containing two Mn atoms is qualitatively similar). We conclude that the FM interaction in nanocrystalline Ge:Mn and GaAs:Mn is *different from* that of the bulk. As noted above, the “host” valence band shifts downward rapidly compared to the Mn d states with decreasing NC size. Below some critical radius, the majority spin Mn d states appear above the top of the valence band [6]. For the size range studied here, the Mn d states form *deep* acceptors. Deep Mn impurities are known to stabilize FM interaction via a double exchange mechanism

involving localized holes, as suggested previously for (Ga,Mn)N [28]. This makes the Mn-Mn interaction essentially a short-range one, consistent with the short-range spin polarization observed in Fig. 1. When we considered two Mn atoms separated by more than one bridging As atom, we found that: (a) such a structure was less stable than the one with a single bridging atom, and (b) the energy differences between the FM and AFM phases decreased rapidly with increasing Mn-Mn separation. This suggests a size-dependent ferromagnetic coupling mechanism, caused by a size-dependent transition from shallow acceptors to deep acceptors.

The lack of ferromagnetism in the ZnSe:Mn NCs is also consistent with the above explanation. In ZnSe:Mn, the t_2 states are fully occupied and there are no holes to which to couple. In bulk ZnSe:Mn, extrinsic acceptor codoping can be used to generate holes that can mediate the Mn-Mn spin interaction [29,30]. To test the applicability of this idea to ZnSe:Mn NCs, we replaced the bridging Se atom with a N atom in the 82-atom NC. This replacement caused the FM configuration to become lower in total energy versus the AFM configuration by 0.20 eV.

In conclusion, we studied the effect of quantum confinement on Mn-containing Ge, GaAs, and ZnSe dilute magnetic semiconductors, by considering the size dependence of their electronic and magnetic properties using first principles calculations. The FM and half-metallicity trends found in the bulk are preserved in the NCs. However, since the Mn states are localized, they are less affected by quantum confinement than are the delocalized host states. As a consequence, in NCs the Mn-related impurity states become much deeper in the gap with decreasing size. This causes the FM stabilization to be dominated by double exchange via localized holes, rather than by free holes or by an RKKY mechanism.

We thank D. Norris and S.-H. Wei for valuable discussions. In Minneapolis, this work was supported in part by the National Science Foundation under DMR-0130395 and DMR-0325218 and the U.S. Department of Energy under DE-FG02-89ER45391 and DE-FG02-03ER15491. In Rehovoth, this work was supported by the Minerva Foundation and a grant from Sir Harry Djangoly (UK). Calculations were performed at the Minnesota Supercomputing Institute, the National Energy Research Scientific Computing Center (NERSC), and the Weizmann Institute's computational materials science supercomputer.

-
- [1] S. A. Wolf, D. D. Awschalom, R. A. Buhrman, J. M. Daughton, S. von Molnar, M. L. Roukes, A. Y. Chtchelkanova, and D. M. Treger, *Science* **294**, 1488 (2001), and references therein.
- [2] L. Bányai and S. W. Koch, *Semiconductor Quantum Dots* (World Scientific Publishing Co. Pte. Ltd., Singapore, 1993), and references therein.
- [3] A. L. Efros and M. Rosen, *Annu. Rev. Mater. Sci.* **30**, 475 (2000).

- [4] D. Loss and D. P. DiVincenzo, *Phys. Rev. A* **57**, 120 (1998).
- [5] M. Ouyang and D. D. Awschalom, *Science* **301**, 1074 (2003).
- [6] S. Sapra, D. D. Sarma, S. Sanvito, and N. A. Hill, *Nano Lett.* **2**, 605 (2002).
- [7] S. Cho, S. Choi, S. C. Korea, Y. Kim, J. B. Ketterson, B. Kim, Y. C. Kim, and J. Jung, *Phys. Rev. B* **66**, 033303 (2002).
- [8] H. Ohno, *Science* **281**, 951 (1998).
- [9] B. Oczkiewicz, A. Twardowski, and M. Demianiuk, *Solid State Commun.* **64**, 107 (1987).
- [10] D. J. Norris, N. Yao, F. T. Charnock, and T. A. Kennedy, *Nano Lett.* **1**, 3 (2001).
- [11] X. Huang, E. Lindgren, and J. R. Chelikowsky, *Phys. Rev. B* **71**, 165328 (2005).
- [12] N. Troullier and J. Martins, *Phys. Rev. B* **43**, 1993 (1991). We used the following s/p/d cutoff radii and partial core radii (in a.u.): Ge: 2.6/2.5/2.8, Ga: 2.99/2.58/2.99 1.76, As: 2.49/2.49/2.49 1.37, Zn: 2.60/2.60/3.60 2.03, Se: 2.60/2.40/3.30 1.25, Mn: 2.3/2.3/2.3 1.1, H: 2.0.
- [13] J. R. Chelikowsky, N. Troullier, and Y. Saad, *Phys. Rev. Lett.* **72**, 1240 (1994).
- [14] S. Blundell, *Magnetism in Condensed Matter* (Oxford University Press, New York, 2001).
- [15] Y.-J. Zhao, T. Shishidou, and A. J. Freeman, *Phys. Rev. Lett.* **90**, 047204 (2003).
- [16] A. Stroppa, S. Picozzi, A. Continenza, and A. J. Freeman, *Phys. Rev. B* **68**, 155203 (2003).
- [17] M. Jain, L. Kronik, J. R. Chelikowsky, and V. V. Godlevsky, *Phys. Rev. B* **64**, 245205 (2001).
- [18] S. Sanvito, P. Ordejon, and N. A. Hill, *Phys. Rev. B* **63**, 165206 (2001).
- [19] L. M. Sandratskii, *Phys. Rev. B* **68**, 224432 (2003).
- [20] T. C. Schulthess and W. H. Butler, *J. Appl. Phys.* **89**, 7021 (2001).
- [21] X. Luo and R. M. Martin, cond-mat/0411394.
- [22] X. Huang (unpublished).
- [23] J. R. Chelikowsky, L. Kronik, and I. Vasiliev, *J. Phys. Condens. Matter* **15**, R1517 (2003).
- [24] M. Linnarsson, E. Janzen, B. Monemar, M. Kleverman, and A. Thilderkvist, *Phys. Rev. B* **55**, 6938 (1997).
- [25] L. Kronik, M. Jain, and J. R. Chelikowsky, *Phys. Rev. B* **66**, 041203 (2002).
- [26] Y. D. Park, A. T. Hanbicki, S. C. Erwin, C. S. Hellberg, J. M. Sullivan, J. E. Mattson, T. F. Ambrose, A. Wilson, G. Spanos, and B. T. Jonker, *Science* **295**, 651 (2002).
- [27] T. Dietl, H. Ohno, F. Matsukura, J. Cibert, and D. Ferrand, *Science* **287**, 1019 (2000).
- [28] T. Graf, S. T. B. Goennenwein, and M. S. Brandt, *Phys. Status Solidi B* **239**, 277 (2003); K. Sato, W. Schweika, P. H. Dederichs, and H. Katayama-Yoshida, *Phys. Rev. B* **70**, 201202 (2004); M. Wierzbowska, D. Sánchez-Portal, and S. Sanvito, *Phys. Rev. B* **70**, 235209 (2004).
- [29] A. Haurly, A. Wasiela, A. Arnoult, J. Cibert, S. Tatarenko, T. Dietl, and Y. M. d'Aubigné, *Phys. Rev. Lett.* **79**, 511 (1997).
- [30] D. Ferrand, J. Cibert, A. Wasiela, C. Bourgognon, S. Tatarenko, G. Fishman, T. Andrearczyk, J. Jaroszynski, S. Kolesnik, T. Dietl, B. Barbara, and D. Dufeu, *Phys. Rev. B* **63**, 085201 (2001).